Master's Thesis

Study for fast scanning with high axial resolution of Lattice light-sheet microscopy

Bo-Kyung Kim

Department of Biomedical Engineering

Graduate School of UNIST

2017

Study for fast scanning with high axial resolution of Lattice light-sheet microscopy

Bo-Kyung Kim

Department of Biomedical Engineering

Graduate School of UNIST

Study for fast scanning with high axial resolution of Lattice light-sheet microscopy

A thesis/dissertation
submitted to the Graduate School of UNIST
in partial fulfillment of the
requirements for the degree of
Master of Engineering

Bo-Kyung Kim

12 / 16 / 2016
Approved by

Advisor
Sung Chul Bae

Study for fast scanning with high axial resolution of Lattice light-sheet microscopy

Bo-Kyung Kim

This certifies that the thesis/dissertation of Bo-Kyung Kim is approved.

12 /16 / 2016

signature

Advisor: Sung Chul Bae

signature

Ha Jin Kim: Thesis Committee Member #1

signature

Jung-Hoon Park: Thesis Committee Member #2

Abstract

Researchers in the optical field have developed light-sheet microscopy to achieve fast scan rates and low photo-toxicity. However, the conventional light-sheet microscopy uses a Gaussian beam or a Bessel beam, so that the resolution in the z-axis direction is not significantly different from the confocal microscope widely used in biology and chemistry. In general, the resolution in the z-axis direction is only about 1/3 of the resolution in the x- and y-directions, although the resolution in the x- and y- direction has been greatly improved for several decades. This is because the side lobe of the light-sheet exists.

Lattice light sheet microscopy overcomes these limitations with thin light sheets using 2D optical pattern. The lattice beam produces a sheet with a much narrower core, which provides a higher axial resolution. Sheet-shaped illumination eliminates out-of-focus fluorescence emissions and enables high-speed imaging with low photo-toxicity. The Lattice light-sheet microscope can construct a low fluorescence background grating beam and all excitation light is within a narrow focus depth. Therefore, light that is out of focus is not irradiated onto the sample, so damage by light is limited to the focal plane. We also provide a high-resolution, high-contrast image of 200 to 1000 images per second.

In this experiment, we will check the performance of Lattice light-sheet microscope complements the disadvantages of conventional confocal microscopy and light sheet microscopy. A sheet-like pattern could be used to create a much thinner light sheet, and it was confirmed that light above the focal plane was gathered higher than the surrounding area. This focuses the fluorescence emission only on the focal plane to prevent further damage to the sample due to phototoxicity of unfocused light. It was also confirmed that the light was uniformly distributed in the light sheet. In addition, when compared to a single-vessel beam light sheet and a lattice light sheet, it was confirmed that the side lobes actually decreased. The fact that the resolution of the Lattice light-sheet microscopy in the z direction corresponds to the range of about 317 nm to 370 nm was confirmed by photographing a fluorescent bead sample.

Contents

List of figures

Nomenclature

3D	3 Dimensional
2D	2 Dimensional
MCCs	Multi Ciliated Cells
ND filter	Neutral-Density filter
AOTF	Acousto-Optic Tuning filter
SLM	Spatial Light Modulator
CCD	Charge-Coupled Device
sCMOS	scientific Complementary Metal–Oxide–Semiconductor
HCG	Human Chorionic Gonadotropin
MBS	Modified Barth's Saline
RDX	1,3,5-Trinitroperhydro-1,3,5-triazine
NA	Numerical Aperture
IFT	Intraflagellar transport
Galvo	Galvanometer, Galvo scanning system
HEPES	4-(2-hydroxyethyl)-1-piperazineethanesulfonic acid
BSA	Bovine serum albumin
pH	Power of Hydrogen
MEM	Minimum Essential Media
DMEM	Dulbecco's Modified Eagle's Medium
ID	Inner Diameter
OD	Outer Diameter

I. Introduction

Confocal microscopes are widely used in biology and chemistry fields because of their ability to perform optical sectioning and 3D high-resolution imaging. A confocal microscope uses pinholes or slits to remove out-of-focus light to improve image quality. However, a significant amount of signal is lost by the pinhole. Also, scanning efficiency is reduced due to optical scattering while scanning a sample with a single beam.[1] Therefore, strong excitation light must be used, which leads to rapid photo-bleaching and high photo-toxicity. Furthermore, due to exposure with excitation light outside the focal plane, the sample already get optical damage before imaging. Even if image quality is not affected by pinholes, tissue damage cannot be prevented.

To overcome these limitations, scientists have developed Light sheet microscopy. Traditional light sheet microscopy is fluorescence microscopy. A thin plane which is only a few micrometers is illuminated perpendicular to the viewing direction. Also, the excited light from the sample is collected by the detector without being reduced signals by the pinhole.[2] This suggests that there is no need to investigate stronger light. As a result, the optical damage and optical damage are reduced considerably. In addition, the light sheet illuminates the cross section at a time, so it has a fast scan speed.[3] A fast scan speed making it suitable for imaging a sensitive sample or a fast process phenomenon. However, the low resolution in the axial direction is still unresolved. Conventional light sheets made with Gaussian beams were too thick compared to cells to be able to perform intracellular imaging.

Eric Betzig developed Lattice light sheet microscopy in 2014.[4] Lattice light sheet microscopy overcomes these limitations by illuminating only a thin section of the sample using light sheets. Ultrathin light sheet is made by using 2D optical lattices. The basic principle of Lattice light sheet is almost the same with traditional Light sheet microscopy, but Instead of using a Gaussian beam, Lattice light sheet microscopy is used the lattice patterned Bessel beam. Lattice patterned Bessel beam produces a sheet with a much narrower core, and this provides high axial resolution.[4] The sheeted illumination eliminates out-of-focus fluorescence emission and allows for high-speed imaging with low photo-toxicity.

In Figure 1, the side lobe of the light-sheet produced by the Bessel beam and the light-sheet produced by the lattice pattern were compared. Here, the side lobe refers to a lobe of a far field radiation pattern except the main lobe. When emitting a radio wave in one direction, the lobe in the target direction has a larger electric field intensity than the other portion. This is called the main lobe. Other lobes, called side lobes, generally represent undesired radiation in unwanted directions. The aperture shows the shape of the beam at the back focal plane of the excitation lens. This shape can be seen immediately after passing through the annular mask. When each beam forms a sheet shape through dithering, it can be seen that the side lobe of a relatively single Bessel beam is broader. This affects the resolution in the z-

axis direction.

Although getting a 3D live-cell imaging with high resolution is ideal in the biological field, high spatial resolution is hard to coexist with high temporal resolution.[5] Increasing spatial resolution requires more time to measure a sample, and also damaging into the specimen such as photo-bleaching and photo-toxicity. However, Lattice light sheet microscopy can construct the low fluorescence background lattice patterned beam, and all the excitation light is within the narrow depth of focus.[4] Therefore, light that is out of focus is not irradiated onto the sample, so that the damage caused by the light is limited to the focal plane. It also provides high-resolution, high-contrast images of 200 to 1000 planes per second.[4]

In this experiment, we will confirmed that lattice light-sheet microscopy can be used for high-speed scanning with the high z-direction resolution. To do this, we try to analyze the performance of the lattice light-sheet microscopy by directly modulating the various beam patterns or by comparing it with the Bessel beam.

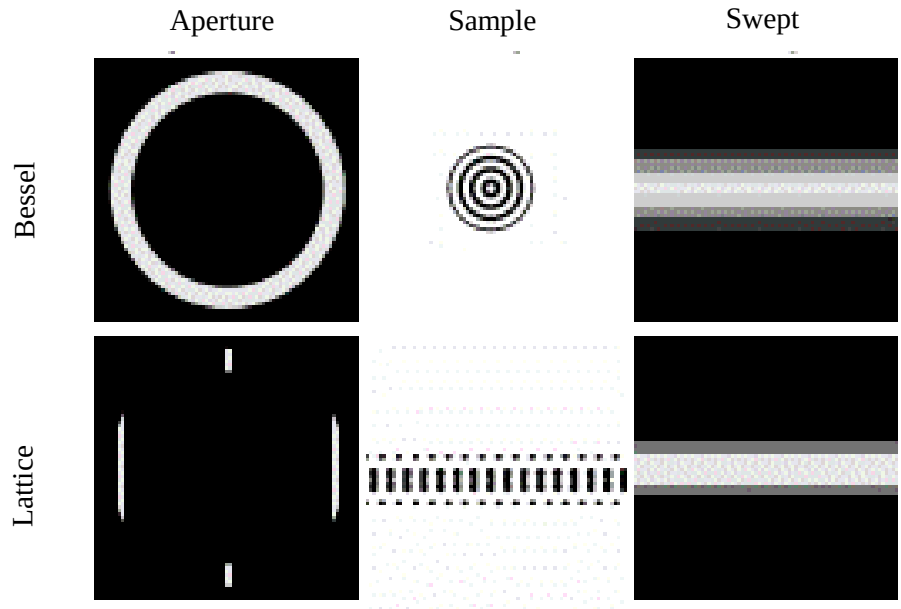

Figure 1. Side lobe comparison between Bessel light-sheet and Lattice light-sheet

II. Experimental Method & Materials

2.1 Optical System Setup

In this system, an overall magnification is 62.5X. We combine 4 diode lasers (405 nm, 488 nm, 570 nm, and 647 nm diode lasers are used.) and use it as a laser source. All components except lasers are mounted on an 18 x 24 inch breadboard. It is erected vertically on an optical table. Laser combiner is on the other breadboard.

2.1.1 Laser combiner system

A schematic diagram of the laser combiner system is shown in Figure 2. It is equipped with 405 nm, 488 nm, 570 nm, and 647 nm lasers. In front of each laser, there is a Neutral-Density filter (ND filter) wheel which can adjust the light quantity physically. It also extends the diameter of the beam with two lenses each. The bandpass filter passes the other laser wavelengths (647 nm, 570 nm, and 488 nm) from the behind, and reflects other wavelengths. The combined light passes through a half-wave plate and an Acousto-Optic Tuning filter (AOTF). An acousto-optic tuning filter is used to select wavelengths and to control strengths of the laser. An acousto-optic tuning filter is also used to synchronize with a spatial light modulator (SLM) that generates a lattice pattern.

2.1.2 Lattice light sheet microscopy system

Figure 3 shows a schematic of an optical path through the Microscope. At first, the linearly polarized beam is entered into the system. A filp mirror, where the beam is first encountered, sends the beam path to the excitation objective lens when the flip mirror is extended. On the other hand, when the flip mirror is folded, it sends light to a wide-field objective lens. Thereafter, a pair of cylindrical lenses extend the input beam in the x direction, and another pair of cylindrical lenses short in the z direction. Finally, the incident light becomes a thin shape. Thus, the thin beam makes to illuminates the Spatial light modulator uniformly with the lattice light sheet pattern displayed. The polarizing beam splitter cube and the half-wave plate provide a phase shift to the diffracted beam. A beam projects to the Spatial light modulator which converts the beam into a lattice pattern. Spatial light modulator is a device that spatially modulates the light beam waveform. Spatial light modulator can quickly render complex patterns. Reflected light from the Spatial light modulator is used to eliminate unwanted diffraction. Creating a

regularly spaced two-dimensional grid and adjusting the period of that grid can cause destructive interference. Lattice light-sheet microscopy uses interference to reduce the intensity of the outer lobe of the Bessel beam.

The figure 5 shows the beam pattern entering the spatial light modulator. A is used in the alignment process with a single-Bessel beam pattern, and B is used in actual imaging with a lattice beam pattern. Each pattern was generated using matlab code. The shape of the beam is actually visible through the Bessel beam camera. The diffracted light passes through a lens with a focal length of 500 mm. This lens allows to focus on a specific pattern on an annular mask with multiple donut-shaped masks printed on it. When the beam passes a transforming lens, the lattice-patterned beam converts to a Fourier diffraction pattern at an annular mask.[10] The annular mask physically filters out the undesired diffracted light as the 0th order and higher order on the Lattice light sheet.[4] After passing through the annular mask, the beam is again demagnified by the pair of lenses.

The figure 6 shows the shape of the annular mask. This annular mask was custom made. We use a mask marked with a red box in this experiment. Twelve annular masks marked with a blue box are suitable for biosample imaging. After that, it is composed of two galvanometers which are driven in the x and z axis directions and a relay lens which forms the 4f system.[11] These galvos are aligned that the reflective light conjugate to the back focal plane of the excitation objective lens.[12] This system allows the sample to be scanned in the x- and z-axis directions. Behind the galvanometer system, there is a beam splitter, which divides the light into two parts: towards the camera and towards the excitation objective lens. This Charge-Coupled Device (CCD) allows you to see the Bessel beam pattern of the beam in the light path. The image of the annular mask is re-magnified to 3.2 times through the relay lenses and it is conjugated to the back focal plane of the excitation objective lens.

When the flip mirror located before the excitation objective lens is folded, the image is formed on another Charge-coupled device. This allows to identify the front aperture of the excitation objective lens. The two Charge-coupled devices mentioned above give help in the align process. Lattice light sheet is projected onto the sample focal plane, and the excited fluorescence is collected by a detection objective lens which is mounted orthogonally with excitation objective lens (Figure 7). The excited fluorescence from the sample passes through a tube lens with a focal length of 500 mm and an emission filter that blocks unwanted wavelength of light. Finally, the image can be detected with a detection scientific Complementary metal–oxide–semiconductor (sCMOS) camera. When you unfold the flip mirror which is located at the beginning of the path of light, the light is directed towards a wide field objective lens. The light passing through the wide field objective lens illuminates the sample from the bottom of the sample. After excitation, the excited fluorescence is passed through a wide field objective lens again and then detected by a CCD located behind a beam splitter. This Charge-coupled devices allows to adjust the position of the sample before detecting the image with the detection camera.

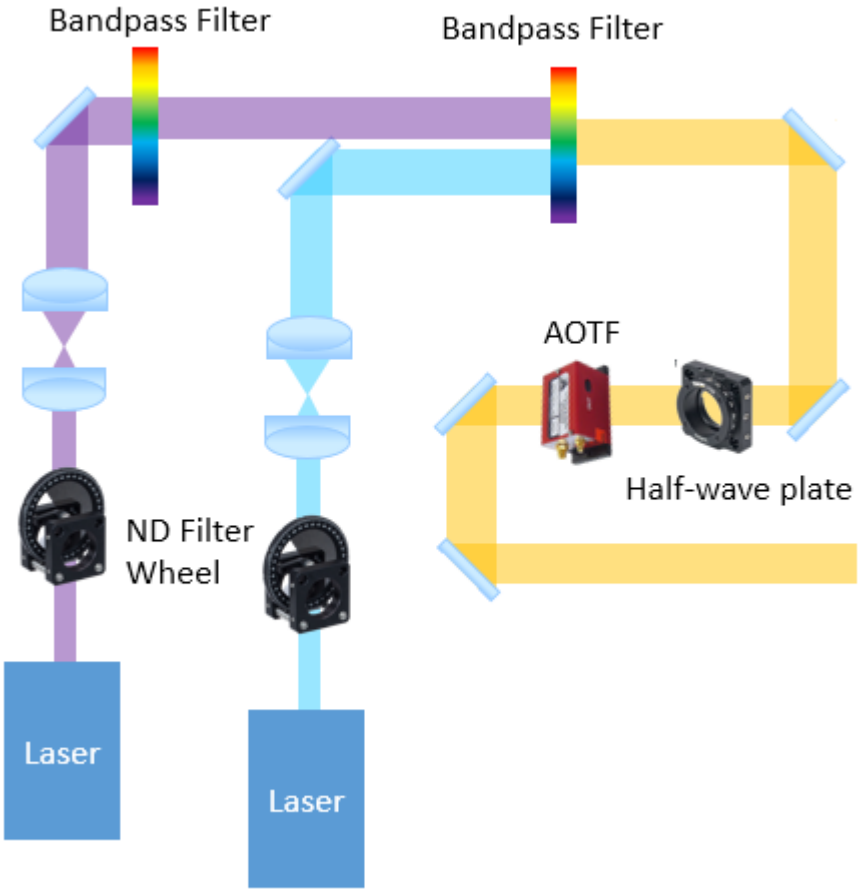

Figure 2. Schematic of an optical path through the Laser combiner.

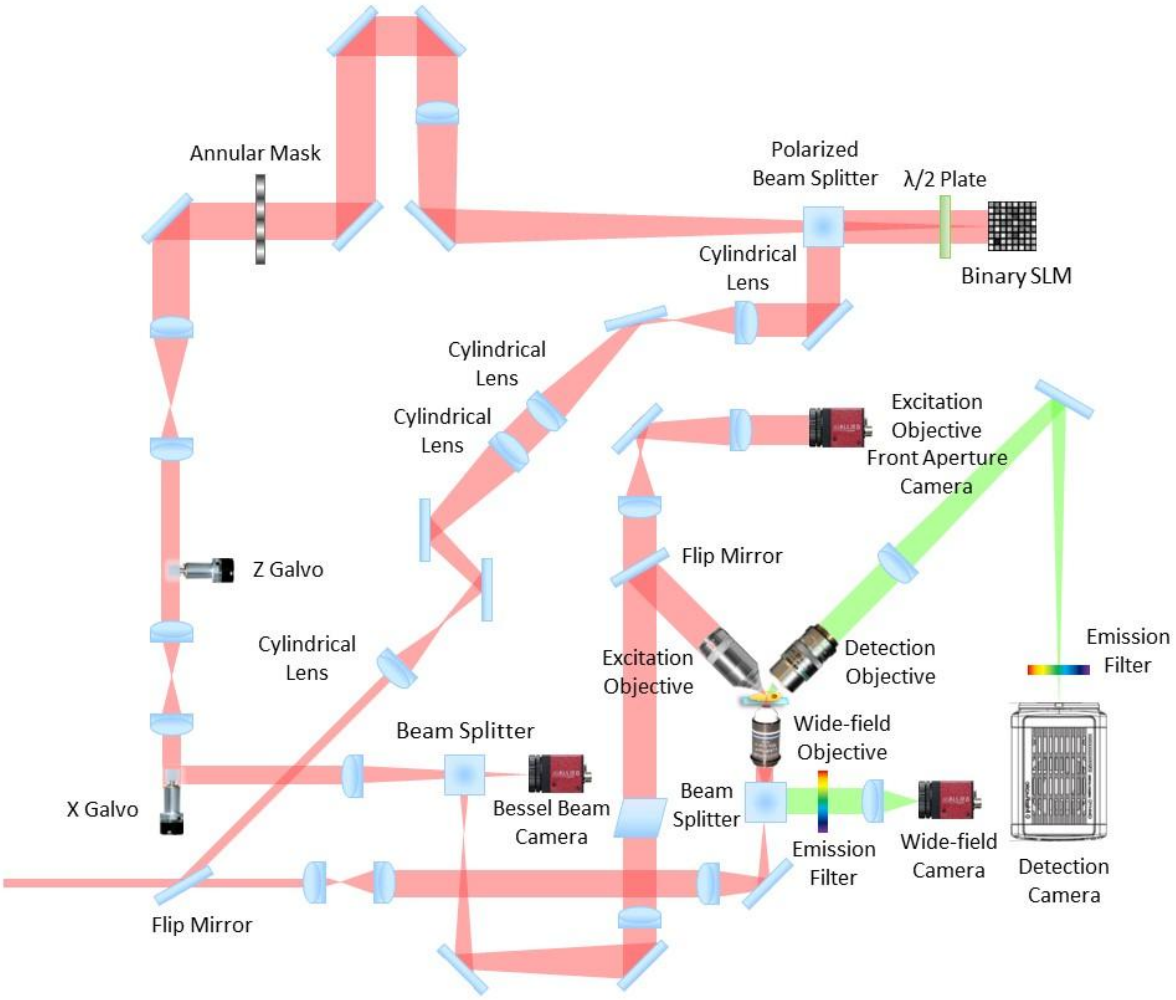

Figure 3. Schematic of an optical path through the Microscope.

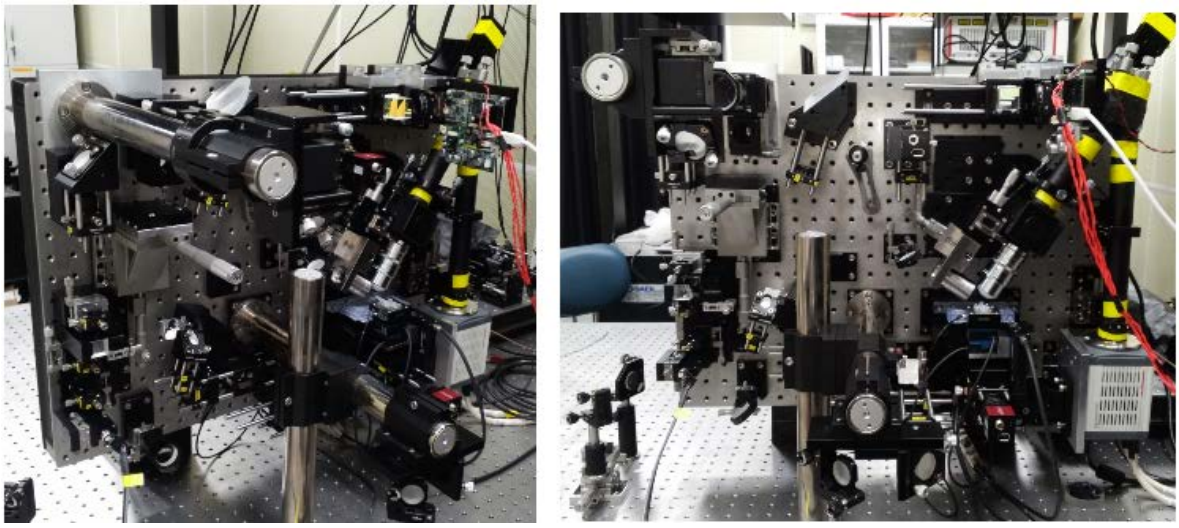

Figure 4 . Actual Lattice light-sheet microscopy system

(A)

(B)

Figure 5. Single Bessel beam pattern and Lattice sheet-typed beam pattern which are loaded on the spatial light modulator.

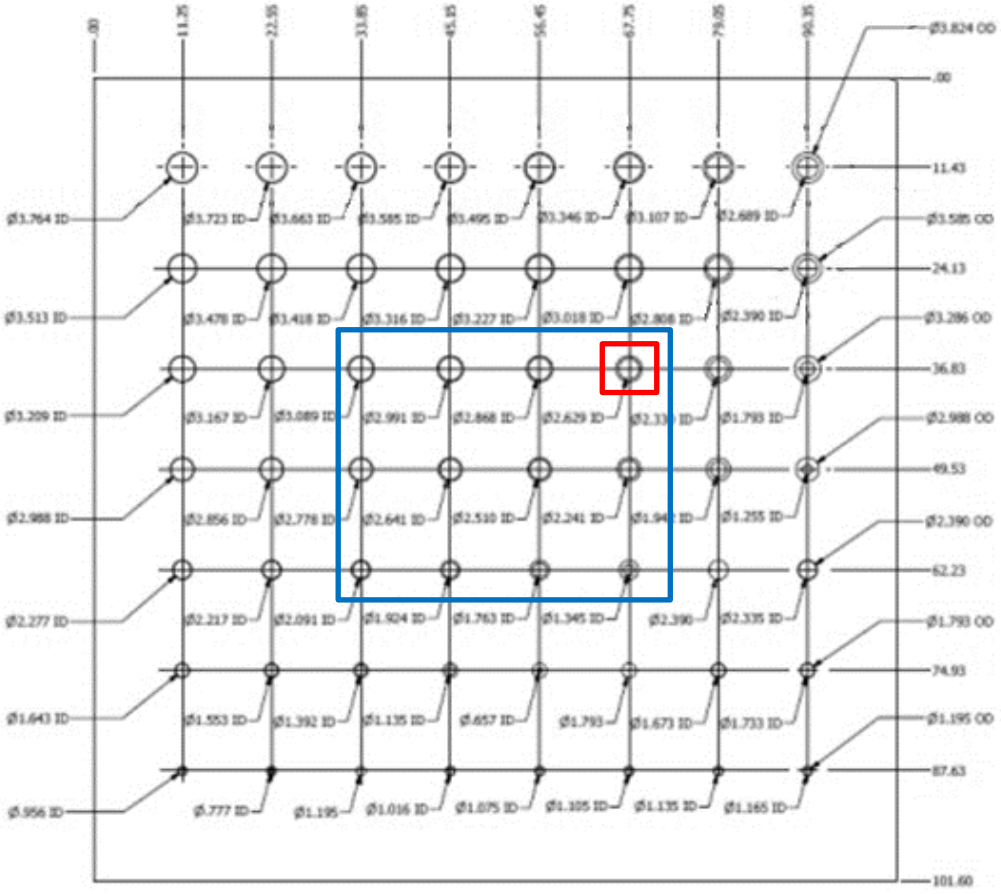

Figure 6. Shape and inner, outer diameter of each annular mask.

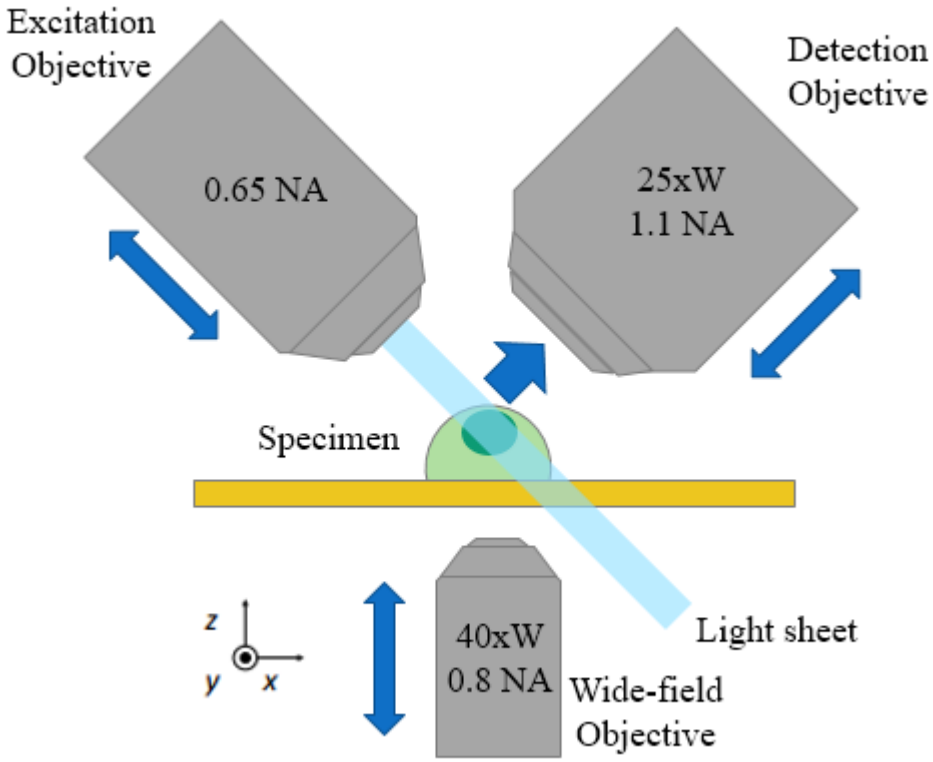

Figure 7. Schematic of three objective lens and light sheet for sample scanning

2.2 Materials preparations for Alignments

2.2.1 Dye solution Preparations

Fluorescein sodium salt was used as dye. It is a water-soluble fluorescent dye and can dissolve 1 mg in 1 ml. The excitation wavelength is 460 nm and the emission wavelength is 515 nm. It is due to permeability due to its small molecular radius. The concentration of the solution should be 2.5 M and kept out of the light.

2.2.2 Fluorescent Beads Sample Preparation

First, cover slip cleaning is required. Remove any debris from the cover slip with distilled water. Then, add 1 M KOH solution and wash on a sonicator for 30 minutes.[13] Discard the KOH solution and wash it 10 times with distilled water. After washing, add distilled water and sonicate for 10 minutes. Add distilled water again and wash 10 times. Dry the cover slip thoroughly when finished. The flueorescnt beads solution should be dropped on it. Fluorescent beads were FluoSpheres® Biotin-Labeled Microspheres, 0.2 μm, yellow-green fluorescent (505/515), and 1% solids. Sonicate for 20 minutes to drop the beads adhering to the container and dilute it to 1: 1000 in distilled water. The diluted beads solution is dropped on the above cover slip by 1μl and heated at 100 ° C to dry the water.

2.3 Imaging process with Lattice light-sheet microscopy

2.3.1 Place sample on sample holder

For sample imaging, we made specimen holders specially. In Figure 8 and 9, it shows a shape of the sample holder and the sample chamber. The sample holder and sample chamber are made of plastic through 3d printing. A 5 mm diameter coverslip can be placed on top of the sample holder. Resize the sample to fit on the top of 5 mm diameter cover slip that if the sample is too bigger than the 5mm diameter cover slip. The cover slip on which the sample is placed is affixed to the sample holder with a weak adhesive or fixed to the sample holder using a clip.

2.3.2 Sample Imaging with Lattie light-sheet microscopy

First, a sample chamber made in a bowl shape is filled with a medium or distilled water. The medium can be either RDX medium or Dulbecco's Modified Eagles's Medium depending on the type of sample. Other transparent culture media are of course possible. This is because the objective lens is a water immersion lens or a water immersion lens. When imaging living cells or tissues, the cells or tissues should always remain in the medium. If the sample does not require special conditions, the experiment will proceed at room temperature. However, if circulatory media is required and a specific temperature is to be maintained, such as using the Eagle’s minimum essential medium or a Dulbecco's modified Eagle medium for cell imaging cultured in a 37 ° C, CO_2 incubator, the system must be modified. Fill the medium instead of distilled water or RDX medium to circulate the Eagle's minimal medium or Dulbecco's modified Eagle's medium using a water bath and water pump. Adjust the sample position by adjusting the x, y, and z-axis sample stages below the sample holder so that the sample is displayed on the detector camera. Obtain images using drive software for lattice light sheet microscopy.

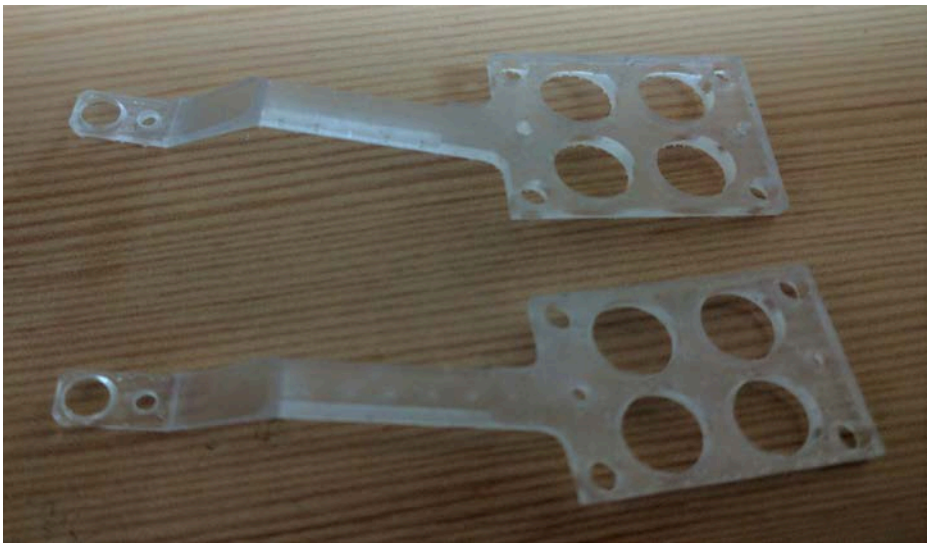

Figure 8. Specially designed sample holder

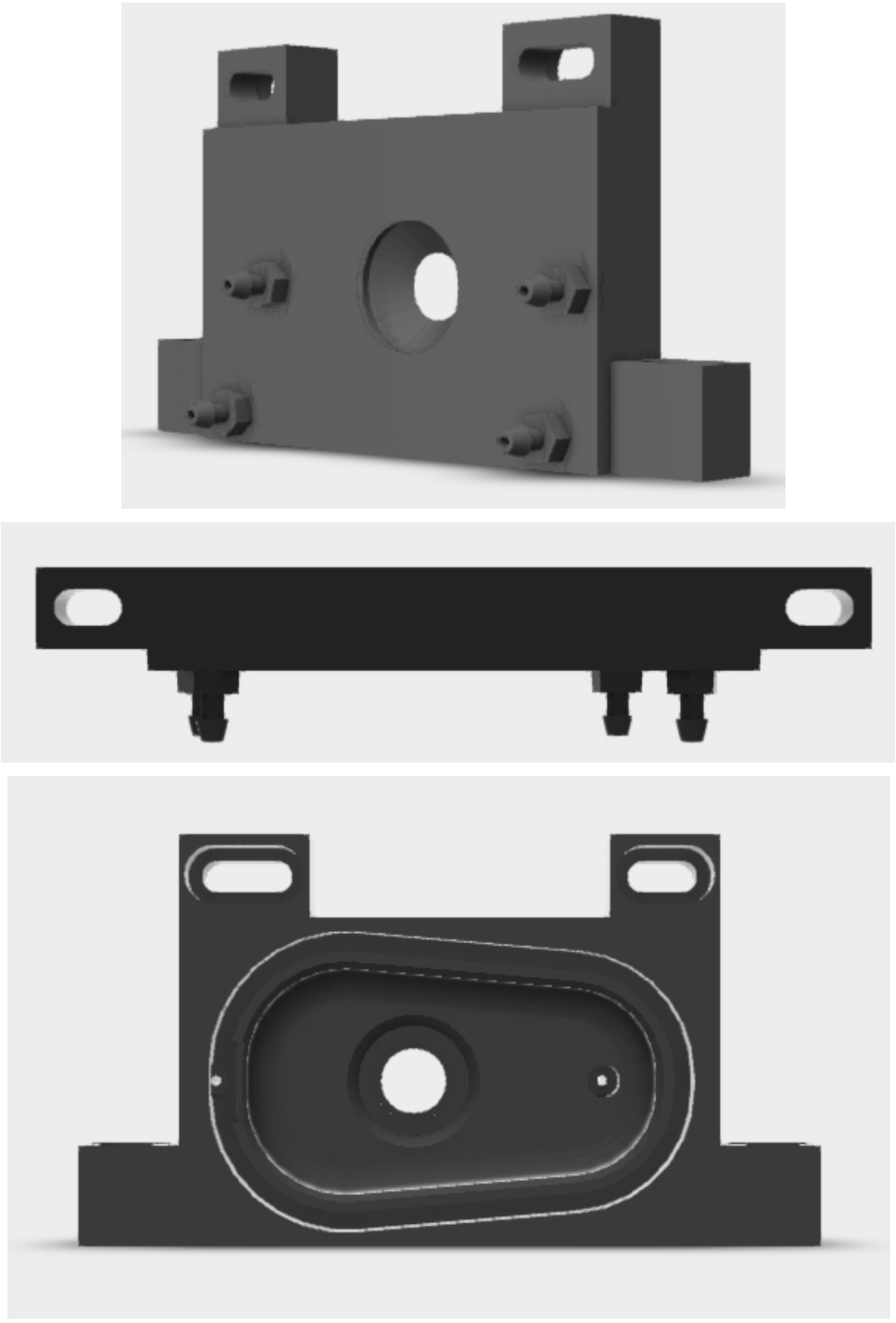

Figure 9. Specially designed sample chamber

3. Results

In Figure 10, we compared the difference between projecting a full pattern and projecting a sheet pattern. When a full pattern is inserted to fill the entire pixels of the spatial light modulator, a relatively thick light sheet is created. The thickness of the light sheet is approximately 15 μm. On the other hand, when a sequence 20 ms sheet pattern is projected according to the annular mask pattern which is 3.585 mm outer diameter and 2.629 mm inner diameter, a relatively thin 5 μm light sheet is produced. In the early part of the system, adjusting the thickness and width of the beam using a set of cylindrical lenses is done to increase the efficiency when the sheet-shaped Spatial light modulator pattern is loaded into the Spatial light modulator. Figure 11 shows the beam pattern at each position in the light path. Figure 11 (A) shows beam with single Bessel beam pattern at the back focal plane of the excitation objective lens. (B) is single Bessel beam pattern at the sample focal plane. It has a uniform pattern by a spatial light modulator and forms a concentric circle. (C) shows a lattice beam pattern at the back focal plane of the excitation objective lens and (D) shows Lattice pattern Beam at the sample focal plane. In (D), the width of the light sheet is about 105 μm and the thickness is about 5 μm.

Next, we compared the intensity profiles of the single bessel beam and the lattice patterned beam. You can see it in Figure 12. Looking at the intensity profile, there is a side lobe that appears as a small peak around the main peak for a single bessel beam. On the other hand, the lattice light-sheet has a relatively small side lobe. This shows that the resolution improvement in the z-axis direction can be expected when imaging with a lattice light-sheet.

Figure 13 shows beam shapes when we illuminate 2.5 μM fluorescein dye solution. Particularly in the case of a single Bessel beam, there is a thin and strong intensity light. Keeping it thin and clear indicates that the light focusses well in the sample illuminating plane. Then we tried to analyze the profile to see if the intensity of the light in that part is actually concentrated. We can confirm that the intensity is actually high in the center of the light.

In the beam alignment process, the image and row profile image of the fluorescein dye solution are taken. (Figure 14) The concentration of the fluorescein salt dye solution is 1.25 μM and the solvent is distilled water. In this figure, we can see the beam image at the time of sample scanning. B represents the row profile of the green box position in A. Since the two distributions must be evenly distributed, align the two row profiles almost exactly. Also, the light sheet should be made thinner by making the overlapping line generated during the crossing of the beam as sharp as possible. This is related to the distance and angle between the excitation objective lens and the detection objective lens. Figures 11 and 12 both use a 488 nm laser wavelength.

Figure 15 shows a fluorescence bead sample taken with a lattice light-sheet microscope. You can see that the shape of the beads looks clean and well. And Figure 15 builds a 3D image by stacking equally

fluorescent beads samples along the z-axis. This is because the beads are not separated well and the signal is strongly detected. These images were taken with a 488nm laser.

In Figure 16, the SLM pattern uses a pattern with sequence 20 ms, 3.585 OD, and 2.629 ID. Camera standard is 256 x 256 pixels, range is 10um, and interval is 0.05um. Z-galvo and z-piezo stages, and the z-axis range is 10 μm, 151 slices, and interval is 0.066 μm. 5 phase step and the phase interval is 0.22. The camera exposure time is 30ms. Because we used 0.2 um of fluorescent beads, we were able to determine the axial resolution of the lattice light-sheet microscopy. We measured the resolution in the z-axis direction through multiple images, and generally had a z-axis resolution in the range of 317 nm to 370 nm.

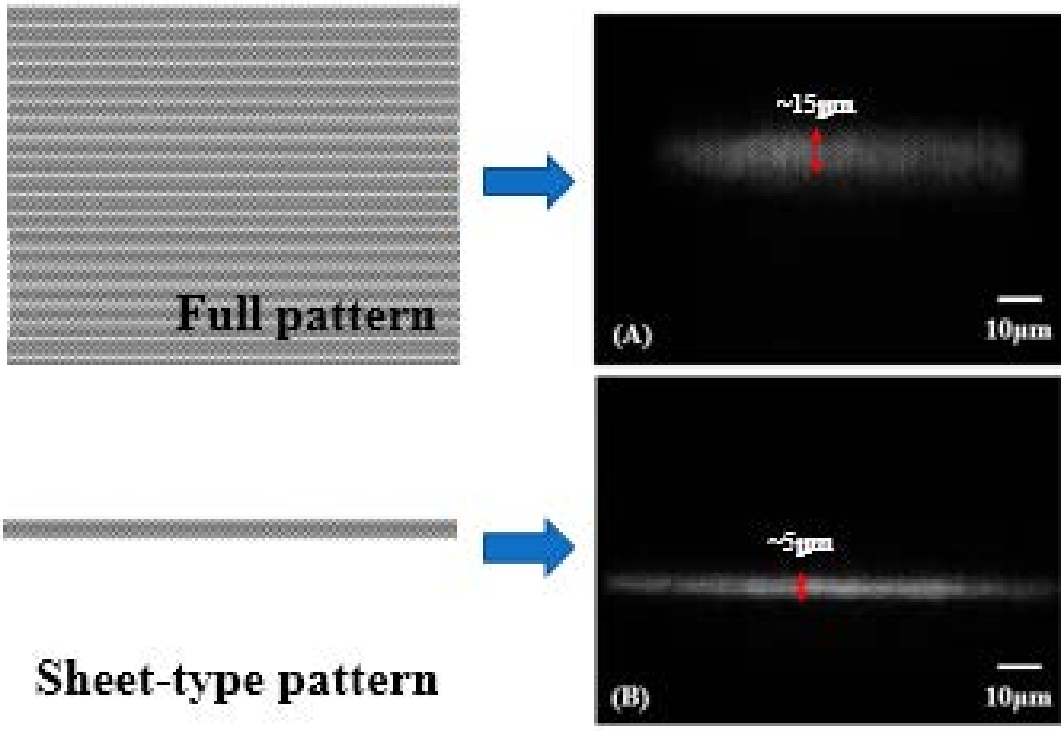

Figure 10. Difference between projected full pattern and projected sheet pattern

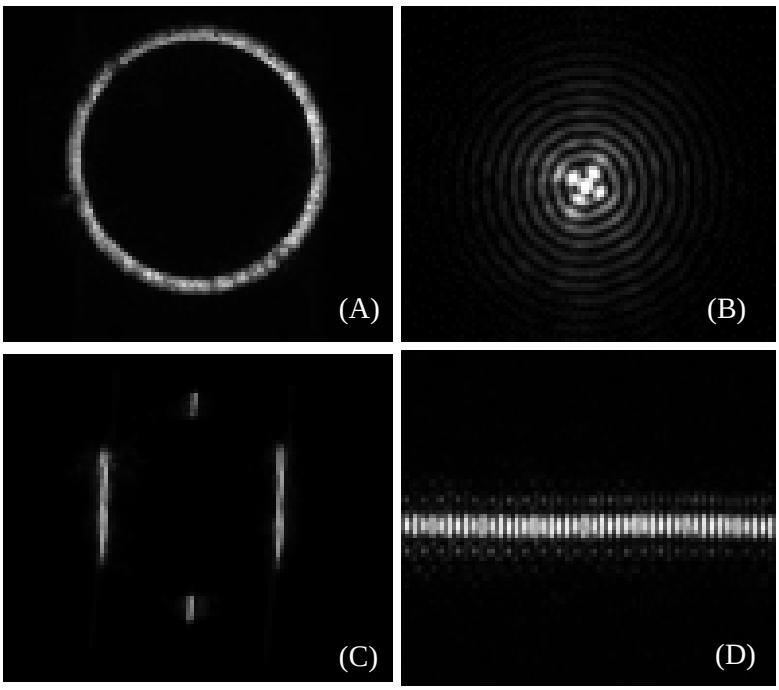

Figure 11. Shape of the single Bessel beam and Lattice Bessel beam along the optical path

(A) Beam with single Bessel beam pattern at the back focal plane of the excitation objective lens.

(B) Single Bessel beam pattern Beam at the sample focal plane.

(C) Beam with lattice beam pattern at the back focal plane of the excitation objective lens.

(D) Lattice pattern Beam at the sample focal plane.

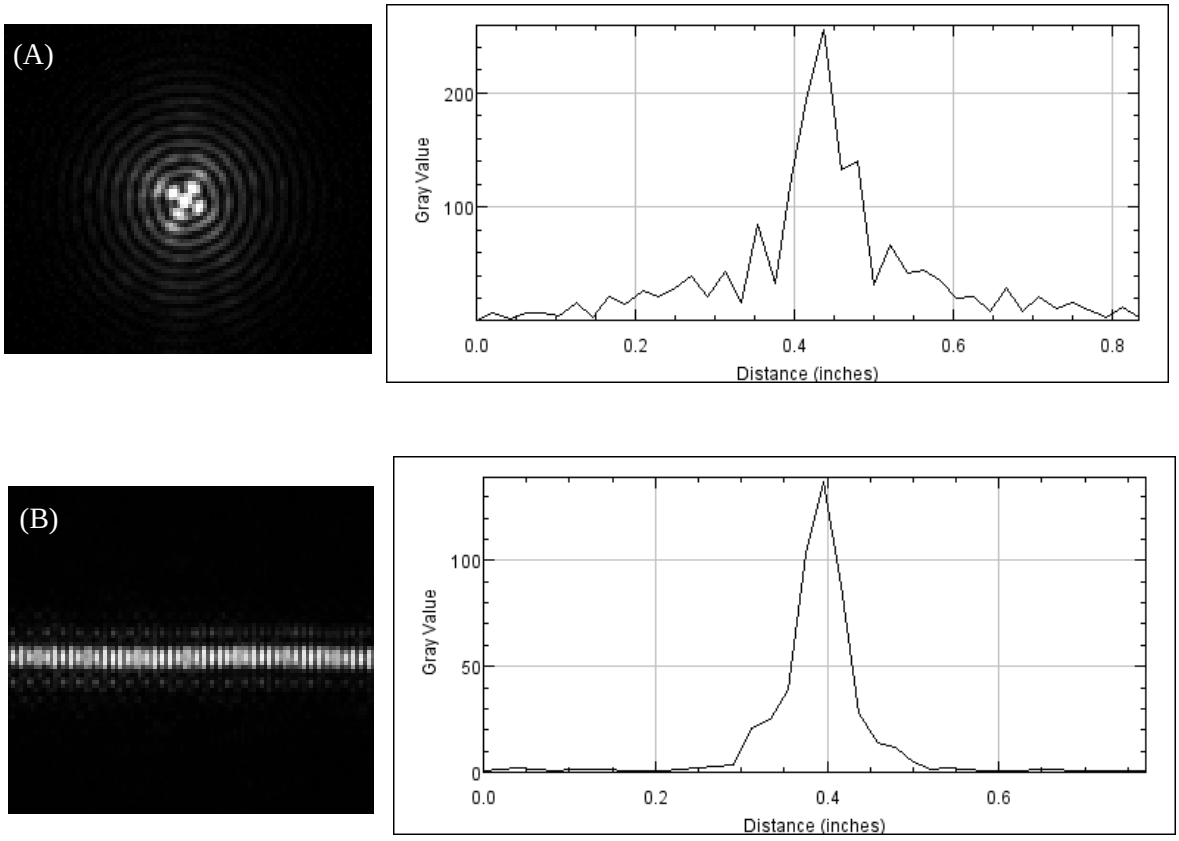

Figure 12. Intensity profile of single Bessel beam and lattice light-sheet

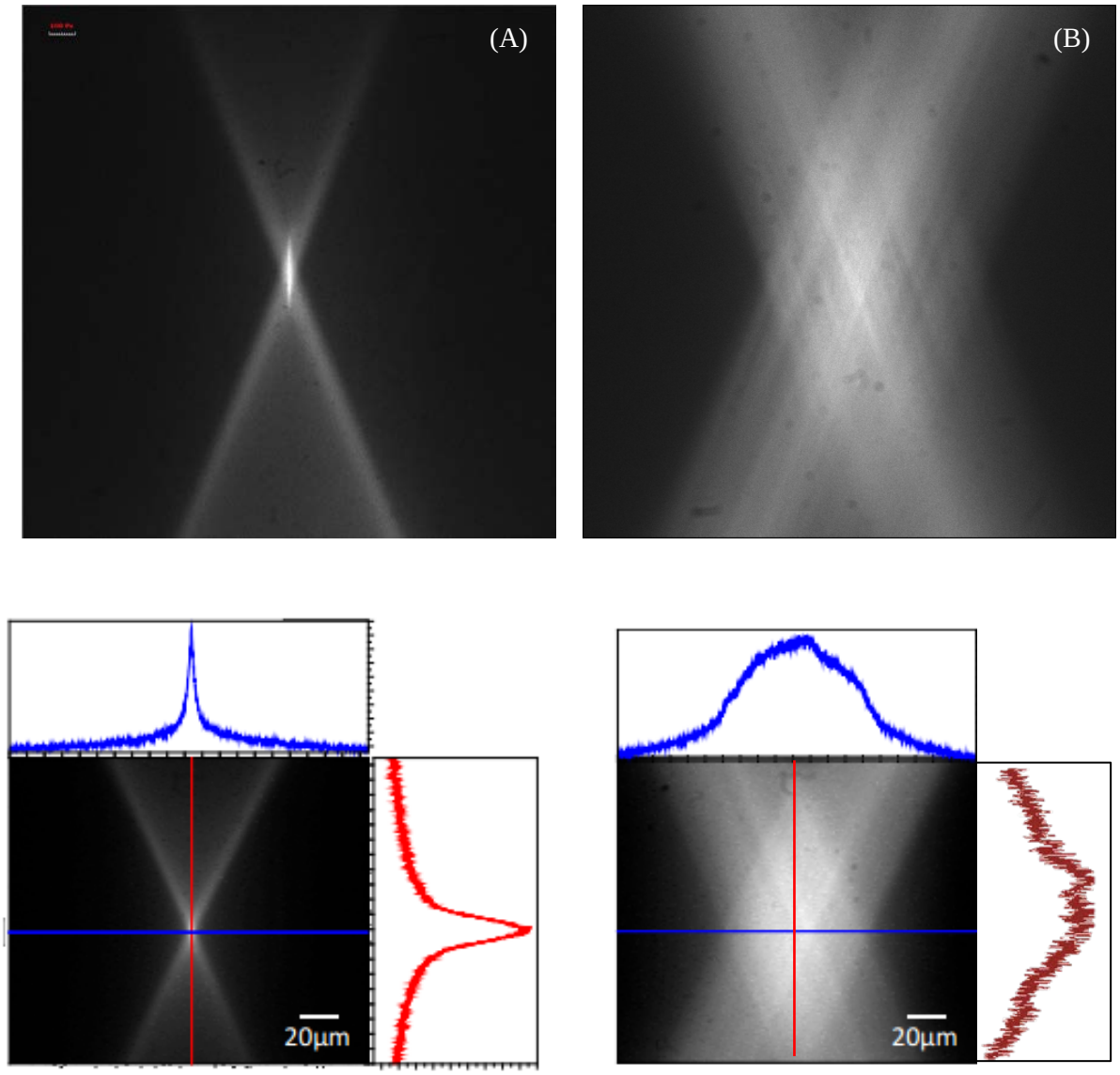

Figure 13. Illuminating dye solution

(A) Single Bessel beam shape of dye solution at sample focal plane

(B) Lattice beam shape of dye solution at sample focal plane

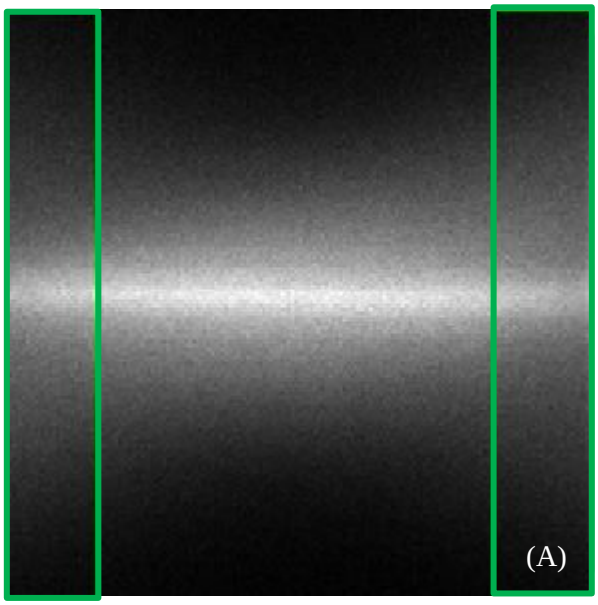

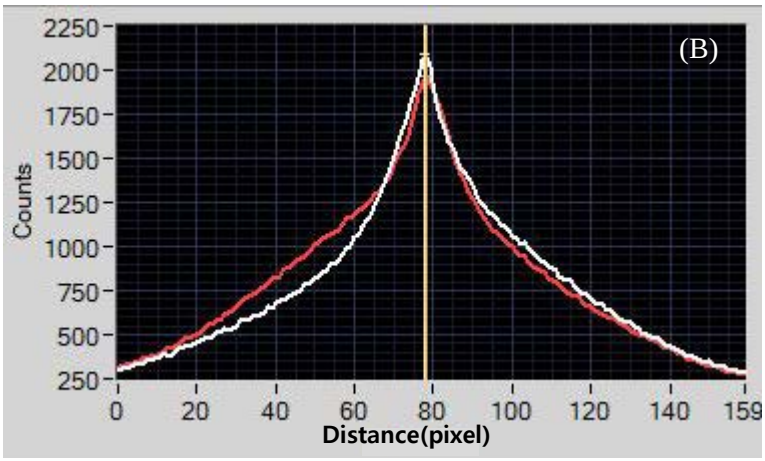

Figure 14. Row profile of the fluorescein dye solution

(A) Magnifying only the center part of figure 12A

(B) Row profile of green box regions of figure 13A

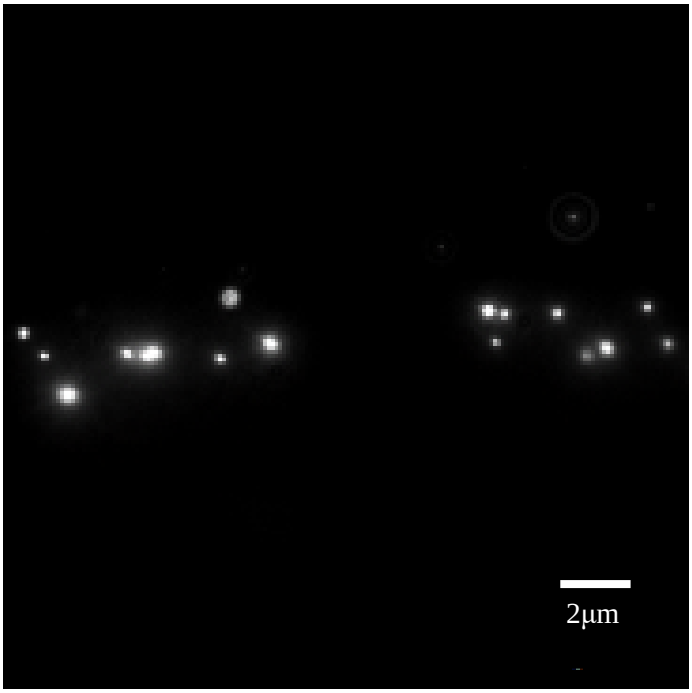

Figure 15. Image of a plane of fluorescent beads

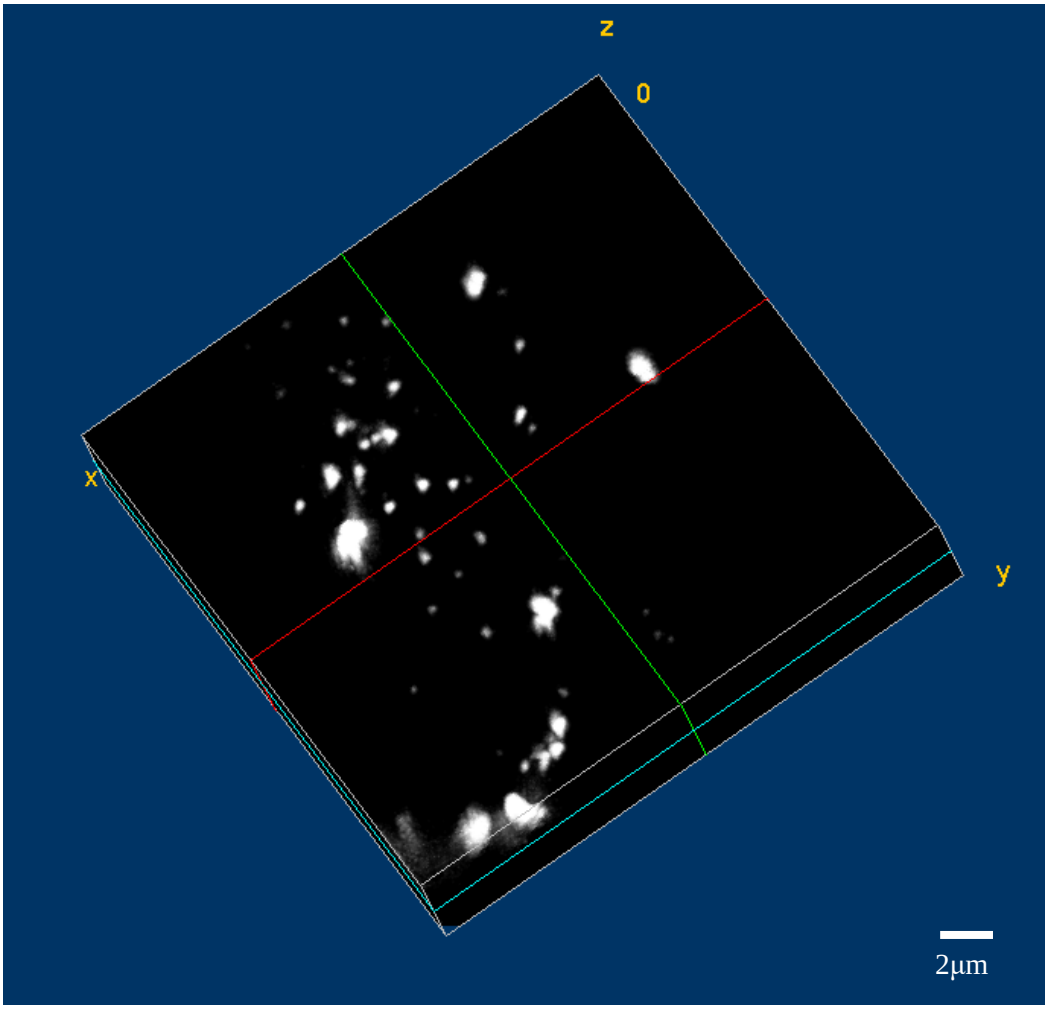

Figure 16. 3 dimensional imaging of fluorescent beads sample

4. Discussion

In the previous experiments, we examined the various capabilities of the lattice light-sheet. Therefore, it is found that fast scanning can be performed with better axial resolution. The lattice light-sheet microscopy has low phototoxicity and low photobleaching as light-sheet microscopy. To maximize all the advantages of a lattice light-sheet microscope, it is time to image living cells, tissues, and living things. Therefore, it will be judged that cilia imaging is performed later, and actually live-cell imaging has better performance than conventional confocal microscope.

For decades, studies on mechanisms of cell behavior and induction and regulation of gene expression have been actively conducted. The reason why the research on this field has been actively carried out in this way, is due to the development of molecular biological techniques and the use of laboratory animals which is suitable for molecular analysis. Xenopus is one of them.

Xenopus, an African amphibian, has many advantages as an experimental animal compared to other amphibians. Current amphibian genetics research is almost dependent on Xenopus. Xenopus is relatively easy to obtain their eggs regardless of the season, and it is possible to breed adults in the laboratory.[6] It is also easy to breed because it grows fast and can withstand external impact. Thus, many molecular genetic studies such as the mechanism of induction and gene expression regulation have been made using this species.

Multi-ciliated cells (MCC) are cilia-rich cells on the surface.[7] It is in the trachea or brain, and it is also in the gonads such as the fallopian tube and the uterus. They acts to control fluid to flow in a certain direction.[8] If these cells do not function properly, serious illnesses can occur. For example, there is a cerebrospinal fluid in the brain that always flows out of the brain. If the cilia in the brain fails to work, the brain spinal fluid will not come out. This causes an increase in intracranial pressure, which leads to hydrocephalus. There are multi-ciliated cells on the surface of the bronchial tubes and some cells without cilia. Cells without cilia play secretory secretion.[9] Scientists are studying the gene and gene expression involved in these multi-ciliated cells, or studying the structure and function of cilia.

To study multi-ciliated cells and clia, it is necessary to see the basal cells, ciliates, cilia and the proteins in cilia. Conventional studies were mainly performed using confocal microscopes. However, since confocal microscopy did not have sufficient high resolution, imaging speed, and imaging range, it was difficult to observe all of them at once. In this experiment, we will suggests that Lattice light-sheet microscope, which complements the disadvantages of conventional confocal microscopy and light-sheet microscopy, may be useful in observing multi-ciliated cells on the bronchial surface.

Multi-ciliated cells (MCCs) control fluid flow in a specific direction. Scientists are studying the gene and gene expression associated with MCCs, or studying the structure and function of ciliates. To study MCCs and cilia, it is necessary to look at basal cells and cilia. Conventional studies have been used

confocal microscopy. However, confocal microscopy did not have sufficient high resolution, image speed, and imaging range, making it difficult to observe everything at once. The imaging speed of the lattice light-sheet microscopy is several hundred planes per second, making it suitable for cilia beating imaging with 20 strokes per second. In future studies, we will image cilia with lattice light-sheet microscopy, and we will image the live embryo by spreading the agrose gels onto the cover slip.

When the sperm penetrates into the egg and the fertilization takes place, the gray crescent rotates by 30 °, and Cleavage occurs.[14] After 2, 4, 8, 16 cell lines, and it becomes morula which have 32 ~ 64 cells. And after more cleavage stage, it becomes blastula which have more than 128 cells. The embryonic development starts with the embryo being slightly cleaved or invagination at the site of the embryo's back. This cleavage becomes a blastopore. The cells that will become the mesoderm in the future move to the inside of the embryo along the edge of the blastopore. Cells that will become ectoderm move along the outside of the embryo. Through this process, the endoderm filled with egg yolk is finally surrounded by ectoderm. As the development progresses, the neural folds are generated from the back of the embryo, and the neural groove which becomes the base of the neural tube is generated. When the neural folds meet at the dorsal midline, a neural tube is formed. Once the neural tube is formed, the neural tube and chorda dorsalis cause differentiation of the surrounding cells. The mesodermal tissue adjacent to the chorda dorsalis becomes somite. The embryo then creates mouth and anus and it finally has a typical tadpole shape.

Fertilized egg can be divided into animal hemispheres and plant hemispheres.[15] This name reflects the motility of the cells, not the real plants and animals. The plant hemisphere is the lower part of the egg where the egg yolk is stored and is used as food for the embryo in development. Animal hemisphere is a pigmented area on the upper part of the egg, and it divides more rapidly than other hemispheres and moves positively.

Animal Cap cells are cells located around the pole of the embryo in the blastula or very early gastrula stage.[16] This tissue becomes a cement gland on the dorsal side of the embryo later. Or it becomes a neurectoderm on the ventral side.

Animal Cap cells are composed of pluripotent cells. Thus it can be induced to form mesodermal or ectodermal cells. This property allows the observation of the activity of various inducers through animal cap cells. By removing the lid of the embryo implanted with the expression structure and analyzing it, it is possible to judge the activity of various genes.

The sample preparation process to be performed later is as follows. Artificial ovulation and artificial insemination; Choose a mature female Xenopus that has not laid eggs within at least three months. These Xenopus laevis are transgenic organisms that express GFP at their membrane. On the day before the experiment, 450IU of Human Chorionic Gonadotropin (HCG) is injected into the dorsal lymph

node,[17] abdominal cavity, or thigh. The day after the injection, lightly press the abdomen to check for ovulation. Once confirmed, the male testes are obtained and disrupted in 1.5 ml of ice-cold 100% Steinberg solution. Drop a drop of sperm suspension on the slide and observe it with a microscope and check the activation level of the sperm. Once the sperm motility is confirmed to be active, keep the sperm suspension cold on ice. Gently press the abdomen of the female xenopus to get eggs in a Petri dish. Dilute the spermicide suspension 20 times with distilled water and spread over the eggs.

Dejelly Xenopus embryo; Place the fertilized egg in a tube and leave a small amount of water enough to lock the egg. Discarding all water can harm eggs. We use stage 9 Xenopus laevis embryo. Add Xenopus embryos in 1x Modified Barth's Saline (MBS). Add the dejelly solution to the embryo with swollen jelly layer and shake gently for 3-5 minutes. This process is dejelly process to strips the jelly layer of the embryo. If the dejelly time is long, the embryo will be damaged, so do not exceed 5 minutes.[18] Discard the supernatant and add 0.1X MBS and wash it up and down. MBS has the osmotic pressure of the frog embryo and serves to clean the embryo without damaging it.

Animal cap cells separation; Remove the vitelline membrane from the dejellied embryo. The Vitelline membrane is located just below the equator. Make sure that only animal cap cells are removed using a sharp tool. Removing only the animal cap cells results in uniform tissue thickness. If the thickness of the tissue is uneven, it means that marginal zone cells have not been removed.[19] Adhering vegetal and yolk cells should be removed immediately. Explant is added to 0.5X Modified Barth's Saline (MBS) and cultured. Cropped Cap cells regain full state within a few hours.[20] Then, animal cap cells are incubated in RDX medium until stage 26. At stage 26, epithelial cells are separated from it and load the isolated cells on the 5mm coverslips. The using medium is RDX medium. This RDX medium contains;

58 mM NaCl, 0.67 mM KCl, 0.34 mM $Ca(NO_3)_2$ $4H_2O$, 0.83 M $MgSO_4$, 3 mM HEPES (4-(2-hydroxyethyl)-1-piperazineethanesulfonic acid), 2 g/L NaHCO, 0.01 % BSA (Bovine serum albumin) and pH 7.4.[21]

5. Conclusion

It has been found that a sheet-like pattern can be used to create a thinner light sheet and the light above the focal plane is condensed higher than the surrounding area. Focusing the fluorescence emission only on the focal plane to prevent further damage to the sample due to the phototoxicity of unfocused light. It was also confirmed that light was uniformly distributed on the sheet. The image speed of the lattice light-sheet microscope is suitable for ciliary images of 20 strokes per second with hundreds of faces per second. In future studies, we will image the cilia with a lattice light-sheet microscope and image the live embryo by spreading the agrose gel onto the cover slip. In this experiment, we will propose that a Lattice light-sheet microscope may be useful for observing live multiple cilia on the bronchial surface.

6. Acknowledgement

We thank Professor Sung Chul Bae for leading the experiment.
We would also like to thank Professor Sang-Hee Shim, who led the experiment in the same way.
We appreciate Professor Tae Joo Park, Professor Tae Joon Kwon and a graduate students of Professor Tae Joo Park, Hyo Jung Shim who offering us the Xenopus animal cap cells samples and gives us active advices about Xenopus imaging.
We thank E. Betzig at Howard Hughes Medical Institute (HHMI), for their microscope and research.
Thanks to A. Chiu and D. Milkie at Colemantech, for their technical expertise.
All resources are funded by Ulsan National Institute of Science and Technology (UNIST).
We also gratefully acknowledge the support of the Janelia Research Center; Especially W. Legant and T. Liu.

REFERENCES

1. Fahrbach, F. O., Gurchenkov, V., Alessandri, K., Nassoy, P., & Rohrbach, A. (2013). Light-sheet microscopy in thick media using scanned Bessel beams and two-photon fluorescence excitation. Optics Express, 21(11), 13824. doi:10.1364/oe.21.013824
2. Benninger, R. K., & Piston, D. W. (2013). Two-Photon Excitation Microscopy for the Study of Living Cells and Tissues. Current Protocols in Cell Biology. doi:10.1002/0471143030.cb0411s59
3. Weber, M., & Huisken, J. (2011). Light sheet microscopy for real-time developmental biology. Current Opinion in Genetics & Development, 21(5), 566-572. doi:10.1016/j.gde.2011.09.009
4. Chen, B., Legant, W. R., Wang, K., Shao, L., Milkie, D. E., Betzig, E. (2014). Lattice light-sheet microscopy: Imaging molecules to embryos at high spatiotemporal resolution. Science, 346(6208), 1257998-1257998. doi:10.1126/science.1257998
5. Liu, Z., Lavis, L., & Betzig, E. (2015). Imaging Live-Cell Dynamics and Structure at the Single-Molecule Level. Molecular Cell, 58(4), 644-659. doi:10.1016/j.molcel.2015.02.033
6. Black, S. D., & Gerhart, J. C. (1985). Experimental control of the site of embryonic axis formation in Xenopus laevis eggs centrifuged before first cleavage. Developmental Biology, 108(2), 310-324. doi:10.1016/0012-1606(85)90035-1
7. Brooks, E., & Wallingford, J. (2014). Multiciliated Cells. Current Biology, 24(19). doi:10.1016/j.cub.2014.08.047
8. Chung, M., Kwon, T., Tu, F., Brooks, E. R., Gupta, R., Meyer, Wallingford, J. B. (2014). Coordinated genomic control of ciliogenesis and cell movement by RFX2. ELife, 3. doi:10.7554/elife.01439
9. Dubaissi, E., Rousseau, K., Lea, R., Soto, X., Nardeosingh, S., Schweickert, Papalopulu, N. (2014). A secretory cell type develops alongside multiciliated cells, ionocytes and goblet cells, and provides a protective, anti-infective function in the frog embryonic mucociliary epidermis. Development, 141(7), 1514-1525. doi:10.1242/dev.102426
10. Mcgloin, D., & Dholakia, K. (2005). Bessel beams: Diffraction in a new light. Contemporary Physics, 46(1), 15-28. doi:10.1080/0010751042000275259
11. Stelzer, E. H. (1990). The Intermediate Optical System of Laser-scanning Confocal Microscopes. Handbook of Biological Confocal Microscopy, 93-103. doi:10.1007/978-

1-4615-7133-9_9

12. Gao, L., Shao, L., Chen, B., & Betzig, E. (2014). 3D live fluorescence imaging of cellular dynamics using Bessel beam plane illumination microscopy. Nature Protocols, 9(5), 1083-1101. doi:10.1038/nprot.2014.087
13. Geertsema, H. J., Duderstadt, K. E., & Oijen, A. M. (2015). Single-Molecule Observation of Prokaryotic DNA Replication. Methods in Molecular Biology DNA Replication, 219-238. doi:10.1007/978-1-4939-2596-4_14
14. Ranzi, S. (1963). The early development of the amphibian embryo at a molecular level. Developmental Biology, 7, 285-292. doi:10.1016/0012-1606(63)90124-6
15. Snook, R. R., Hosken, D. J., & Karr, T. L. (2011). The biology and evolution of polyspermy: Insights from cellular and functional studies of sperm and centrosomal behavior in the fertilized egg. Reproduction, 142(6), 779-792. doi:10.1530/rep-11-0255
16. Animal Cap Isolation from Xenopus laevis. (2007). Cold Spring Harbor Protocols, 2007(12). doi:10.1101/pdb.prot4744
17. Henriques, U. (1964). Breeding Of Xenopus Laevis Daudin. European Journal of Endocrinology, 45(4 Suppl). doi:10.1530/acta.0.045s089
18. Henry G., Brivanlou I., Kessler D., Hemmati-Brivanlou A., Melton D. (1996) TGF-β signals and a prepattern in Xenopus laevis endodermal development. Development 122:1007–1015.
19. Lamb T.M., Knecht A.K., Smith W.C., Stachel S.E., Economides A.N., Stahl N., Yancopolous G.D., Harland R.M. (1993) Neural induction by the secreted polypeptide noggin. Science 262:713–718.
20. Sive, H. L., Grainger, R. M., & Harland, R. M. (2007). Dejellying Xenopus laevis Embryos. Cold Spring Harbor Protocols, 2007(10). doi:10.1101/pdb.prot4731
21. Harata, A., Matsuzaki, T., Ozaki, K., & Ihara, S. (2013). The Cell Sorting Process of Xenopus Gastrula Cells Progresses in a Stepwise Fashion Involving Concentrification and Polarization. CellBio, 02(02), 54-63. doi:10.4236/cellbio.2013.22007